



Published in final edited form as:

Neuroinformatics. 2010 December ; 8(4): 213–229. doi:10.1007/s12021-010-9077-7.

Identification of Imaging Biomarkers in Schizophrenia: A Coefficient-constrained Independent Component Analysis of the Mind Multi-site Schizophrenia Study

Dae Il Kim,

The Mind Research Network, 1101 Yale Boulevard NE, Albuquerque, NM 87131, USA

Jing Sui,

The Mind Research Network, 1101 Yale Boulevard NE, Albuquerque, NM 87131, USA

Srinivas Rachakonda,

The Mind Research Network, 1101 Yale Boulevard NE, Albuquerque, NM 87131, USA

Tonya White,

Department of Psychiatry, University of Minnesota Medical Center, Minneapolis, MN 55454, USA

Dara S. Manoach,

Neuroimaging Division, Department of Psychiatry, Massachusetts General Hospital, Charlestown, MA 02129, USA

V. P. Clark,

The Mind Research Network, 1101 Yale Boulevard NE, Albuquerque, NM 87131, USA.

Department of Psychiatry, University of New Mexico, Albuquerque, NM 87131, USA

Beng-Choon C. Ho,

Department of Psychiatry, University of Minnesota Medical Center, Minneapolis, MN 55454, USA

S. Charles Schulz, and

Department of Psychiatry, University of Minnesota Medical Center, Minneapolis, MN 55454, USA

Vince D. Calhoun

The Mind Research Network, 1101 Yale Boulevard NE, Albuquerque, NM 87131, USA.

Department of Psychiatry, University of Minnesota Medical Center, Minneapolis, MN 55454, USA.

Department of Electrical Engineering, University of New Mexico, Albuquerque, NM 87131, USA

Dae Il Kim: dkim@mnrn.org; Vince D. Calhoun: vcalhoun@unm.edu

Abstract

A number of recent studies have combined multiple experimental paradigms and modalities to find relevant biological markers for schizophrenia. In this study, we extracted fMRI features maps from the analysis of three experimental paradigms (auditory oddball, Sternberg item recognition, sensorimotor) for a large number ($n=154$) of patients with schizophrenia and matched healthy controls. We used the general linear model (GLM) and independent component analysis (ICA) to extract feature maps (i.e. ICA component maps and GLM contrast maps), which were then

© Springer Science+Business Media, LLC 2010

Correspondence to: Dae Il Kim, dkim@mnrn.org; Vince D. Calhoun, vcalhoun@unm.edu.

Information Sharing Statement

The CCICA toolbox can be downloaded from (http://icatb.sourceforge.net/fusion/fusion_startup.php) along with a sample feature dataset. To obtain information regarding access to the actual feature maps and fMRI datasets used in this study, please contact the corresponding authors.

subjected to a coefficient-constrained independent component analysis (CCICA) to identify potential neurobiological markers. A total of 29 different feature maps were extracted for each subject. Our results show a number of optimal feature combinations that reflect a set of brain regions that significantly discriminate between patients and controls in the spatial heterogeneity and amplitude of their feature signals. Spatial heterogeneity was seen in regions such as the superior/middle temporal and frontal gyri, bilateral parietal lobules, and regions of the thalamus. Most strikingly, an ICA feature representing a bilateral frontal pole network was consistently seen the ten highest feature results when ranked on differences found in the amplitude of their feature signals. The implication of this frontal pole network and the spatial variability which spans regions comprising of bilateral frontal/temporal lobes and parietal lobules suggests that these regions might play a significant role in the pathophysiology of schizophrenia.

Keywords

Schizophrenia; Coefficient constrained independent component analysis; Independent component analysis; fMRI; Biomarkers; CCICA; Working memory; Auditory oddball; Sensorimotor

Introduction

One of the major goals in schizophrenia research involves finding a meaningful biological marker that can aid in its diagnosis and further clarify its pathophysiology. We define a biological marker as a consistent quantitative neuroimaging marker that can accurately characterize schizophrenia. In this regard, functional magnetic resonance imaging (fMRI) has been widely used to probe the underlying brain activity that might distinguish schizophrenia patients from a matched control group. Various paradigms have been implemented to specifically test particular sensory and cognitive processes in the brain. These include, but are not limited to the processing of infrequent auditory stimuli (Kiehl et al. 2005b), working memory (Goldman-Rakic 1994), sensorimotor processes (Schroder et al. 1999), and resting state paradigms (Broyd et al. 2008). These studies have produced a rich collection of potential biomarkers, but few studies have delved into the potential “cross-information” between them. In other words, commonalities which exist across these biological markers might provide a more stable cognitive marker for schizophrenia that might not be easily realized by analyzing results from a single task. Our study attempts the exploitation of this joint-information by utilizing a recently developed method known as coefficient-constrained independent component analysis (CCICA) (Sui et al. 2009a) on a large number of features generated from two popular analysis approaches: the general linear model (GLM) (Friston 1994) and independent component analysis (ICA) (Calhoun et al. 2001)

The GLM relies on the convolution of a canonical hemodynamic response with the experimental paradigm to generate a predicted brain response. This predicted response is then regressed against the preprocessed fMRI dataset at every voxel within the brain, resulting in a statistical map that depicts a set of brain regions which are highly correlated with the experimental task. These statistical maps are often referred to as contrast images and the comparison of these maps in schizophrenia patients and matched controls have been the basis for a large number of fMRI studies in schizophrenia (Glahn et al. 2005; Hill et al. 2004; Kindermann et al. 1997). ICA has a significantly different approach and instead makes the assumption that the raw fMRI timecourse is a linear mixture of spatially independent components. The spatial component maps that are created are often interpreted as functional connectivity maps and have also been labeled in this context as temporally coherent brain networks (Calhoun 2007a, b). These networks have been shown to be affected in schizophrenia (Garrity et al. 2007; Kim et al. 2009a), suggesting that functional

connectivity between brain regions can represent another characteristic source for its pathology. Our analysis takes both the contrast maps from SPM and the component maps from ICA as a set of potential neuroimaging biomarkers. Our goal with CCICA then is to find and exploit the joint information in these features that best separates schizophrenia patients from our matched healthy controls.

Many neuroimaging studies have used a common set of tasks to probe potential disease-related biomarkers in patients with schizophrenia and our analysis took advantage of this consistency. In light of this trend, the National Institute of Mental Health's strategic plan for psychopathology has promoted the use of basic tasks in their attempt to diagnose mental illness (<http://www.nimh.nih.gov/research-funding/rdoc.shtml>). One commonly used task has been the auditory oddball discrimination (AOD) task. For schizophrenia patients, a noticeable and consistent reduction in the P300 event-related brain potential relative to matched controls during the detection of a distinct auditory stimuli have suggested the importance of this task in potentially elucidating a meaningful biomarker (Ford 1999). Furthermore, this task is often used as a robust measure of brain activity (Kiehl et al. 2005a) and significant differences in schizophrenia have been found using both a GLM and ICA approach (Kiehl et al. 2005b; Kim et al. 2009b). Another common task found in studies related to schizophrenia is the maintenance and manipulation of working memory (WM) processes. The consistency of WM deficits appearing in patients with schizophrenia (Lee and Park 2005) including their first-degree relatives (Meda et al. 2008), has led to the use of the Sternberg item recognition paradigm (SIRP) (Sternberg 1966) to probe these cognitive deficits (Manoach 2003). A large multi-site analysis of this task for patients with schizophrenia has shown deficits in multiple networks that included regions of the default-mode network along with areas associated with WM such as the dorsolateral prefrontal cortex (DLFPC) (Kim et al. 2009a). Finally, many previous studies have focused on sensorimotor gating in schizophrenia to study disease-related cognitive deficits during the execution of simple hand movements along with an auditory stimulus. The sensorimotor task designed for this purpose is a simple block design task has been known to robustly engage the motor and auditory regions of the brain (Machado et al. 2007). This task was also successful in finding relevant biomarkers that aided in the classification of patients with schizophrenia (Sui et al. 2009a). Our study extracted features from all three tasks using ICA and GLM from a large number of patients with schizophrenia and matched controls ($n=154$) as part of the Mind clinical imaging consortium (MCIC).

The goal of this study was to implement and extend a recently developed algorithm (CCICA) by applying it to a larger and feature rich MCIC fMRI dataset to determine group-discriminative brain regions associated with schizophrenia. As mentioned briefly before, what makes CCICA uniquely suited to finding potential biomarkers is due to its incorporation of group information as a prior, making it sensitive to potential group differences that might exist across these features. Thus, the normal ICA estimation process of maximizing independence also attempts to maximize a group difference criterion, which in our case is a modified t-statistic. More generally, CCICA is attempting to find areas in the brain that tend to covary uniquely, but discriminately between patients and controls. The discriminative patterns that it finds are referred to as independent components and depict a set of brain regions that reflect a group-discriminative biological marker. Based off of previous fMRI studies that utilized CCICA (Sui et al. 2009a) as well as other studies that have attempted to classify schizophrenia patients from controls (Calhoun et al. 2007a, b), our hypothesis was that CCICA will locate and isolate regions within the prefrontal cortex, thalamus, and bilateral temporal lobes as major group-discriminative regions. Furthermore, we believed that there would be a strong consistency in the type of features that are highly ranked in their group-discriminative scores for both J-divergence and p-value metrics.

Methods

Participants

Schizophrenia patients along with their matched healthy controls provided written informed consent for the Mind Clinical Imaging Consortium. Healthy controls were free from any Axis 1 disorder, as assessed with the Structured Clinical Interview for DSM-IV-TR (SCID) screening device. Patients met criteria for schizophrenia in the DSM-IV based on the SCID and a review of the case file by experienced raters located within each site. All patients were stabilized on medication prior to the fMRI scan session. Participants were recruited from four sites and these were the University of New Mexico (26 Patients/29 Controls, Ratio (patients/controls): 0.9), University of Minnesota (25 patients/21 Controls, Ratio: 1.19), University of Iowa (8 Patients/24 Controls, Ratio: .33), and Massachusetts General Hospital (9 Patients/12 Controls, Ratio: .75). The mean duration of illness for patients was found to be 9.125 years, with a standard deviation of 9.91 years.

Patients and controls had significant differences in the participant level of education, but no significant differences in the level of parental or maternal education. WRAT scores showed significant IQ differences between the two groups. Patients and controls had no differences in age or handedness. Symptom scores were determined using the schedule for the assessment of positive symptoms (SAPS) (Andreasen 1984) and negative symptoms (SANS) (Andreasen 1983). This information including handedness and gender can be found in (Table 1).

Auditory Oddball Discrimination Task

The AOD task has been used to determine significant differences in the sensory processing of infrequent auditory stimuli for patients with schizophrenia. The participant is presented with a continuous sequence of three distinct stimuli ('targets', 'novels', and 'standards') and asked only to press a button with their right index finger whenever they hear a 'target' stimuli. Target and novel stimuli are infrequent and occur with a probability of $p=0.09$ each. Standard stimuli occur more frequently with a probability of $p=0.82$. Target stimuli are represented as 1.2 kHz tones, standard stimuli as 1 kHz tones, and novel stimuli as complex computer generated sounds. Each stimulus is presented with a pseudorandom order and lasts for 200 ms, with an inter-stimulus interval that randomly varies between 550–2,050 ms (mean=1,200 ms). A total of four runs were acquired per session and each run comprised of 90 stimuli. The sequences for target and novel stimuli were exchanged between runs to balance their presentation across all four runs.

Sternberg Item Recognition Paradigm (SIRP)

The SIRP is a block design task that assesses the maintenance and scanning components of working memory. Each block consists of four phases and begins with an instructional cue, which displays the word 'learn' for 1 s. This is followed by an encode phase, which begins the presentation of a memory set composed of one, three, or five digits, constituting three levels of WM load (low 1 L, medium 3 L, high 5 L). The probe phase follows afterwards, where a single digit is presented, and for each digit probe, the participant is asked to respond. The participant is asked to respond with a right trigger press if the digit is a member of the memorized set or a left trigger press if it is not. Finally a fixation phase appears where the subject is instructed to relax to prepare for the next trial. The duration of this fixation phase is random, changing between 4–20 s. Six blocks (two blocks of each of the three WM conditions) constitute a run and each run lasts approximately 6 min.

Sensorimotor (SM)

The SM task is used to find robust differences in the sensory processing of auditory and motor coordination for patients with schizophrenia. The task is an on/off block design with a 16 s duration for each block. The 'on' block consists of 200 ms tones presented with a 500 ms stimulus onset asynchrony. A total of eight tones were played during the 'on' block in ascending and descending cycles with the 'off' block following the completion of these eight tones. The participant was required to press a button with their right thumb after each tone and this task was repeated twice in the scanner with each session lasting approximately 4 min in duration.

Imaging Parameters

Scanning was performed across four sites: the University of New Mexico (UNM), University of Iowa (IOWA), University of Minnesota (MINN), and Massachusetts General Hospital (MGH). All sites, except for UNM, utilized a Siemens 3 Tesla Trio Scanner, while UNM utilized a Siemens 1.5 Tesla Sonata. The scanners were equipped with a 40 mT/m gradient and a standard quadrature head coil. The fMRI pulse sequence parameters were identical for all three tasks (AOD, SIRP, SM) and were the following: single-shot echo planar imaging (EPI); scan plane=oblique axial (AC-PC); time to repeat (TR)=2 s; echo time (TE)=30 ms(3 T)/40 ms(1.5 T); field of view (FOV)=22 cm, matrix=64 × 64; flip angle=90 degrees; voxel size=3.4 × 3.4 × 4 mm³; slice thickness=4 mm; slice-gap= 1 mm; number of slices=27; slice acquisition=ascending.

Data Analysis: Pre-processing

Datasets were preprocessed using SPM5. Realignment of fMRI images were performed using INRIAlign, a motion correction algorithm unbiased by local signal changes (Freire et al. 2002). Datasets were then spatially normalized into the standard Montreal Neurological Institute (MNI) space using an echo planar imaging template found in SPM5 and slightly subsampled to 3 × 3 × 3 mm³, resulting in 53 × 63 × 46 voxels. Finally, spatial smoothing was performed with a 9 × 9 × 9 mm³ full width half maximum Gaussian kernel.

Feature Extraction: General Linear Model

For each individual task, a GLM approach was used to create maps which reflected the degree to which each voxel exhibited task-associated variation which were then used as features within our CCICA analysis. Specifically, a separate GLM analysis was performed for each task (AOD, SIRP, SM) and consisted of a univariate regression of the timecourse at each voxel with an experimental design matrix, generated by the convolution of the task onset times with a hemodynamic response function. This resulted in a set of beta-weight maps associated with each parametric regressor for each task. The subtraction of one beta-weight map with another is often referred to as a contrast map, which represents the effect of a task in relation to an experimental baseline.

For our purposes, we were interested in the relative effect of target or novel stimuli versus standard stimuli in the AOD task, the average probe effect or the average encode effect for the SIRP task, and the sensorimotor response for the SM task. More specifically, the target versus standard contrast in the AOD task attempts to capture the BOLD response associated with responding to the 1.2 kHz target noise which engages the cognitive processes associated with attention orientation followed by a motor response in the form of a button press. The novel versus standard contrasts attempts to capture the BOLD response associated with irrelevant stimuli and fMRI studies have shown the benefit of using these particular contrasts in elucidating the pathophysiology of schizophrenia (Laurens et al. 2005). The average probe contrast in the SIRP task is associated with the combined effect

(low, medium, and high WM load) of recalling correctly the WM items that were presented recently during the task. The average encode contrast represents a similar design, except it attempts to model the blocks associated with the incorporation of the SIRP digits into WM for all three conditions. Finally, the sensorimotor task is a simple block contrast that measures the relative effect of a continuous motor tapping response to a simple repetitive tone to the experimental phase where no motor-tapping or sound stimuli were presented.

Feature Extraction: Independent Component Analysis

A group spatial ICA was performed using infomax algorithm (Bell and Sejnowski 1995) within the GIFT toolbox v1.3d (<http://icatb.sourceforge.net>). We estimated the optimal number of components for ICA by using a modified minimum description length algorithm (Li et al. 2007), which was found to be 19 for the AOD task, 23 for the SIRP task, and 22 for the SM task. Since ICA with infomax is a stochastic estimation process, the end results are not always identical. To remedy this, we applied ICASSO (Himberg et al. 2004) to our initial ICA analysis which allowed us to reiterate our ICA analysis for 20 iterations and to utilize the centroid of the resulting spatial maps. The spatial maps and their respective timecourses were calibrated to z-scores. The features selected for our CCICA analysis were comprised of eight components that were highly similar across our three tasks (Fig. 1), containing activation patterns seen from previous ICA studies of fMRI. The overlay of the ICA components in Fig. 1 are all maps generated from a one-sample t-test of their respective component maps for all subjects and further thresholded at $p < 1 \times 10^{-12}$ (False Discovery Rate corrected). The SPM contrasts maps are also the results of a one-sample t-test thresholded at various p-values beyond $p < 1 \times 10^{-4}$ (False Discovery Rate corrected) for display purposes. A full listing of the features selected for both ICA and GLM, along with their respective descriptions can be found in (Table 2).

Coefficient Constrained Independent Component Analysis (CCICA)

For a full technical description of CCICA and its analytical assumptions, we refer the reader to these references (Sui et al. 2009a, b). CCICA is a modification of a traditional ICA algorithm using infomax. The traditional group ICA algorithm has been widely applied to a number of fMRI studies (Beckmann et al. 2005; Calhoun et al. 2008) and is used here to extract our initial features for CCICA. ICA attempts to extract a set of maximally independent signals from a set of recorded signals that are assumed to represent their linear mixture. In regards to fMRI, these recorded signals are the preprocessed fMRI datasets, and the independent components it extracts results in a set of spatially distinct set of brain regions along with an associated ICA timecourse. CCICA however is significantly different in that the traditional ICA cost function of maximizing independence now incorporates a group discriminative cost, represented as a squared t-statistic. In other words, by providing prior information to the algorithm as to which datasets are controls versus patients, the extraction of components by independence can now be modified to also favor group differences.

It is important to note that CCICA is currently implemented on second-level features, after extraction of those features via ICA and GLM, rather than the original fMRI datasets. Thus, it attempts to delineate meaningful group-discriminative patterns that might be seen across features generated from a variety of analysis techniques (i.e, GLM, ICA) and across various tasks (AOD, SIRP, SM). The approach that CCICA takes is similar to the first-level analysis using ICA, but with a few caveats. The data-reduction step that is normally utilized via PCA is modified in CCICA to better preserve the group-discriminative information that would normally be lost otherwise. This modified algorithm is termed principal component analysis with reference (PCA-R). An overview of the analysis steps used in this study can be seen in graphical form in (Fig. 2).

The steps of our analysis can be delineated as follows. Five GLM and twenty four ICA features were extracted from our first-level GLM and ICA analysis. Following feature extraction, we reshaped these features from both groups with a general modification of the classic ICA model $X = AS$, extended as:

$$\begin{bmatrix} X_h \\ X_p \end{bmatrix} = \begin{bmatrix} A_h \\ A_p \end{bmatrix} \cdot S$$

Where the observed data X consists of stacked features (single or pairwise) along subjects with dimensions $N \times L$ (subjects by voxels) while subscripts h and p refer to healthy controls and patients respectively. A is the mixing coefficient matrix with subscripts identical to X . S is an $M \times L$ matrix, where M is the number of independent sources specified for our study to be 12. The number of independent sources was chosen based off of a previous CCICA study by (Sui et al. 2009a)

Following our specified number of components, we utilized PCA-R, for our data reduction step. The canonical PCA, which is often used in the first-level analysis of fMRI data using ICA, transforms data into an orthogonal coordinate system so that the components are sorted by their variance. Since the components which contain the largest variance are not necessarily sensitive to group differences, PCA-R is a modification of PCA that incorporates the mean group difference as a categorical variable for sorting. Its specific details can be found in these studies (Caprihan et al. 2008; Sui et al. 2009a). CCICA is followed by data-reduction via PCA-R. The goal of ICA is to find the unmixing matrix $W=A^{-1}$ (ignoring the permutation and scaling ambiguity) so that the source estimation of $U = WX$ is as close as possible to the true source S . Furthermore, the cost function associated with classical ICA is the maximization of independence across the sources often denoted as the objective function H . CCICA modifies this cost function by including the sum of the squared T statistic of the constrained component(s):

$$C=H+\lambda \sum T_i^2$$

where λ is a constraint weight associated with the t-statistic T and i is the index of the constrained component. Maximization of the cost function C is based off the gradient ascent algorithm, widely used in searching for the local optima of a function. Like the extraction of the first level ICA features, CCICA utilizes Infomax for its ICA algorithm and this has been shown to be optimal if the nonlinearity used to find independence is closely matched to its source density via maximum likelihood.

Automatic Artifact Removal

Once CCICA is completed, an automated artifact removal algorithm was utilized to filter results that showed a significant correlation with cerebrospinal fluid and physiological noise. The algorithm we used was identical to the approach used in (Sui et al. 2009a) which utilized an approach that automatically labeled the components of interest according to two criteria. The first criterion determined a spatial correlation with the CCICA derived component with a grey matter and a ventricular cerebrospinal fluid template. If the correlation with the grey matter template was significantly less than the correlation with the ventricular cerebrospinal fluid, the component was considered to be artifactual and discarded. The second criterion calculated a metric called the focusing degree, which is defined by the ratio between the spatial entropy and clustering degree of the resulting component. If the spatial entropy is high and the clustering degree is low, the component is

considered artifactual. For more information regarding the specific details related to this algorithm, we reference the reader to Sui et al 2009a.

Optimal Component Selection

CCICA was performed on a single and pairwise combination of the 29 unique features selected from our first-level analysis. This resulted in a total of 406 possible pair-wise comparisons along with the individual analysis of the 29 features for a total of 435 single/combinatorial results. The substantial number of results requires an appropriate metric to determine which feature/component pairing represents a relevant biomarker. For our study, we calculated two metrics that were also used in the first study that implemented CCICA. The first was a p-value generated from a two-sample t-test between the resulting mixing matrix coefficients of patients and controls. This metric allows us to quantify the probability that both groups showed a significant difference in the modulation of their feature signal. The second was a J-divergence score which intuitively represents the degree to which the spatial distribution of a feature(s) differed between two groups. The J-divergence is formally defined as the symmetric form of the Kullback-Leibler (KL) divergence, where the KL divergence measures the amount of extra information needed to encode a true distribution P given an approximate distribution Q.

$$D_{KL}(P \parallel Q) = \sum_i p(x_i) \ln \frac{p(x_i)}{q(x_i)}$$

In the field of information theory, this extra “information” can be thought of as the number of extra “bits” required in order to represent our true distribution using Q and thus when P and Q are equivalent, the KL-divergence will become zero. The symmetric form of this measure that we use, known as the J-divergence, can be seen below:

$$D_J = \frac{1}{2} D_{KL}(P \parallel M) + \frac{1}{2} D_{KL}(Q \parallel M)$$

$$M = \frac{1}{2}(P + Q)$$

Here M represents the average distribution between P and Q. The motivation for using the J-divergence metric is to avoid the assumption of labeling the control or patient group as representing the “true” distribution. A higher J-divergence reflects a larger difference between controls and patients on the joint histogram distribution of U_h and U_p as mentioned above. A graphical representation of this difference can be seen from our results in Fig. 5. The previous study by Sui et al. 2009a, b, utilized a J-divergence threshold of 1.5, and due to the significantly larger number of subjects in our sample, we focused only on results with a minimum threshold for the p-value as $p = 1.0 \times 10^{-4}$ and a J-divergence score of 2.5, which allowed us to report only the most discriminating components. For our results, we only focus on the top 2 components, which reflect a J-divergence greater than 3.5.

Results

Behavioral Findings

The AOD task showed no significant differences between patients and controls in the percent accuracy of target responses, reaction time to targets, and number of misses. A small, but significant difference was seen for the number of incorrect hits, where patients were greater than controls. For the SIRP task, significant differences were seen across all WM loads in the percent accuracy of target responses, but both groups averaged greater than 95% across all loads. There were no significant differences for the overall reaction time (Table 3). Due to the simplicity of the SM task, no behavioral information is reported for this study.

CCICA Results

The top ten components ranked on their p-values and J-divergence scores can be seen along with their associated t-statistics (Table 4). However, due to the substantial number of these results, we report and discuss the top two feature components that showed the lowest p-values and the two highest J-divergence components. Figures 3 and 4 depict the regions that are implicated in these components with a threshold of $z > 2.5$ for the lowest p-values and highest J-divergences respectively. We show in Tables 5 and 6 the most significant brain regions associated with these top feature components, list the size of their respective activation areas, and the maximum z-scores within their particular brain region.

The J-divergence score represents the degree to which the spatial distribution of the CCICA activation differs between patients and controls for that component. In other words, the divergence measure provides us with some information regarding the spatial variability associated with a particular CCICA component and the degree to which they differ between patients and controls. Figure 5 shows a graphical representation of what this difference in the spatial distribution might look like for the top J-divergence component (ICA SM DMN2 & SPM AOD Targets). The p-value reflects a between-group difference with regards to the mixing matrix coefficients, which can be interpreted as a difference in the amplitude of their feature signals. The sign of the t-statistic, found in Table 4 refers to a two-sample t-test where controls are assumed to be greater than patients. Thus, a negative t-score represents a direction in which the sample mean is greater for patients than controls in regards to their mixing matrix coefficients and the regions that are implicated can be seen in Figs. 3 and 4.

Top P-value Components

The two CCICA components that showed the most significant p-values consisted of a joint feature combination (ICA SM Temporal & ICA SM Frontal Pole) and a single feature component (ICA SM Frontal Pole). The ICA SM Temporal component engaged regions in the bilateral temporal lobes, while the ICA SM frontal pole engaged primarily areas in the superior and middle frontal gyrus. Following this joint component, the SM ICA frontal pole feature was also found to be the second highest ranked component. Unsurprisingly, the regions engaged in this feature component were highly similar to the SM frontal pole found from the previous joint component, with differences isolated to the extent of their spatial distribution. The top ten CCICA components were dominated by a few features and notably the SM ICA frontal pole was found in all of the top ten components, followed by networks associated with the primary visual area (V1) and temporal lobe networks. Except for the joint feature component that consisted of the ICA AODV1 and ICA SM frontal pole networks (J-Div=1.99), none of these components contained high J-divergence scores (J-Div<1). Finally, the t-statistic associated with these top 2 components were negative, suggesting that the activation amplitude associated with those areas were greater in patients with schizophrenia than controls.

Top J-divergence Components

In regards to the J-divergence between groups, the top component (J-div=4.19) featured a joint combination between the ICA SM DMN2 and an SPM AOD target contrast map. The SM DMN2 feature uniquely implicated regions in the middle and superior temporal gyrus while the AOD target feature exclusively engaged regions in the superior and inferior parietal lobule. Both features showed the medial frontal gyrus as playing a significant role, but the AOD target feature implicated a significantly larger portion of this area. The next highest J-divergence (J-div=3.99) was seen in a joint component between the ICA AOD frontal pole network and an ICA SIRP primary visual network. Both feature components contained regions associated with bilateral temporal lobes as well as the post central gyrus. The SIRP V1 feature uniquely engaged frontal regions of the brain such as the middle and superior frontal gyrus. On the other hand, the AOD frontal pole feature found regions in the thalamus and insula. Unlike the components that showed highly significant p-values, more heterogeneity was seen in the features combinations and their associated regions.

Discussion

In order to elucidate potential biomarkers for schizophrenia, our study analyzed a large number of subjects and extracted a total of 29 fMRI features for each subject, which were further analyzed using CCICA. The resulting CCICA components were filtered using an automated artifact removal tool and then ranked based off of their p-values and j-divergences. By taking a data-fusion approach, we hoped to exploit the potential “cross” information that existed between various tasks to determine which biological markers would best discriminate between schizophrenia patients and controls. From the results of our analysis, our most striking finding was seen in the component features associated with the most significant p-values. After filtering, the top ten CCICA components all contained a frontal pole ICA component network from the SM task. The J-divergence results reflected a significant, but different aspect of potential biomarkers in schizophrenia. The top 2 components in this regard implicated a varied, but well defined set of brain regions that have often been linked to schizophrenia. This included areas such as the superior/middle temporal gyrus, superior/inferior parietal lobules, and superior/middle frontal gyrus. We found that our results were consistent with our hypothesis of prefrontal dysfunction, but also noticed a significant heterogeneity in the spatial variability of patients with schizophrenia as assessed using our J-divergence scores.

One of the major strengths of this analysis was the incorporation of a various number of functional feature maps and their joint combinations to determine group-discriminative biological markers. Thus, from a total of 29 possible features, it was encouraging to see a single feature type dominate our p-value rankings, specifically the SM frontal pole ICA network. The consistency of this frontal pole network suggests a number of implications for schizophrenia. First, prefrontal dysfunction in schizophrenia has been well-delineated as a consistent area of pathology for a number of years, supported by many fMRI and structural MRI studies using a variety of approaches (Goldman-Rakic and Selemon 1997; Manoach 2003; Meisenzahl et al. 2008). Secondly, the p-value metric determines the extent to which the amplitude of a feature component signal differs between patients and controls. This contrasts with the j-divergence metric which assesses the degree to which the spatial distribution of the feature component differs between the two groups. From this perspective, our CCICA analysis suggests that prefrontal dysfunction in schizophrenia might represent a strong potential biological marker which might be related more to the modulation of its activity rather than any significant differences in its spatial specificity. The t-statistics associated with these components were negative, suggesting greater activation in schizophrenia patients than healthy controls. Evidence in fMRI data for hyper/hypo frontality in schizophrenia has been mixed and the issue is currently unresolved

(Minzenberg et al. 2009). However multiple studies have shown a hyperfrontal response in schizophrenia, especially during working memory tasks. Experimental paradigms that test WM processes inside the fMRI scanner have shown hyperfrontality areas such as the posterior parietal regions (Quintana et al. 2003), ventrolateral prefrontal cortex in first episode patients (Schneider et al. 2007) and dorsal lateral prefrontal cortex (Manoach 2003). Finally, an ICA component nearly identical to the frontal pole component featured in our analysis was significantly different in schizophrenia patients during an auditory oddball task (Kim et al. 2009b). In that study, a large-scale ICA analysis was performed and controls showed a greater positive modulation of the component's ICA timecourse relative to patients. This particular component was considered to be the most statistically significant of the eight components that passed the study's p-value threshold.

The CCICA components that reflected the greatest J-divergence scores depict a set of well known regions that have been previously implicated in schizophrenia. The ICA DMN2 component from the sensorimotor task and the AOD frontal pole feature component engaged significant areas of the superior and middle temporal gyrus. These regions have been closely linked to the successful processing of auditory stimuli and their dysfunction has been related to the auditory hallucinations that often plague patients with schizophrenia (Barta et al. 1990; Pearlson 1997). Our results are also consistent with a previous CCICA study that used an identical analysis approach and found the highest ranked J-divergence component to prominently contain bilateral temporal lobes (Sui et al. 2009a). Furthermore, regions of the medial and superior frontal gyrus were shown to be significantly affected in the top 2 components associated with our high J-divergence measures. The medial and superior frontal gyrus play a prominent role in the characterization of this disorder; its impairment often connected to a dysfunction in executive processes (Davidson and Heinrichs 2003; Minzenberg et al. 2009). Looking more closely at the group specific spatial maps for the top J-divergence component (Fig. 5), it can be seen that patients and controls recruit a significantly different set of brain regions associated with their respective feature maps, suggesting that spatial heterogeneity might be a significant aspect of schizophrenia.

The J-divergence results suggest a correlation with the reported grey matter volumetric differences found in structural MRI studies of schizophrenia. Affected regions such as the superior/middle temporal gyrus, the superior/inferior parietal lobule, and the frontal gyrus from our top 2 components represent a widespread, but consistent set of regions which have shown grey matter volume abnormalities in schizophrenia. Considering that the J-divergence score is associated with the spatial distribution of these feature maps, there might be considerable overlap between these regions and morphometric brain volume studies in schizophrenia. Specifically, the superior and middle temporal gyri along with the thalamus have been one of the most common regions for grey matter differences in meta-analyses of structural MRI studies for schizophrenia. Structurally based studies that have used alternative methods of analysis such as ICA have also found significant reductions in the thalamus and inferior parietal lobes for patients with schizophrenia (Xu et al. 2009). This finding of a more variable localization of correlated activation within the patient group could reflect greater variability in the gross morphology (Park et al. 2004) and/or functional organization of the involved regions on the basis of neurodevelopmental abnormalities. It might also reflect the use of more variable strategies to accomplish the tasks. This finding is consistent with prior work that has shown greater heterogeneity in the location of peak fMRI activation (Manoach et al. 2000) and more variable patterns of functional connectivity during working memory tasks in schizophrenia patients compared to controls (Meyer-Lindenberg et al. 2001). Though it is possible that grey matter volume reductions might not necessarily affect the functional brain activity associated with those regions, a number of studies (Antonova et al. 2005; Calhoun et al. 2006) have reported that a significant link

might exist and further studies that fuse MRI and fMRI data together might help better elucidate this relationship.

Our results also seem to not only favor specific brain regions, but also a particular experimental paradigm. The SM task was represented in all of our top ten feature combinations when ranked by p-values and fifty percent when ranked on J-divergence scores. The reasons for the SM task to be the most effective paradigm for extracting these group-discriminative components is not entirely clear, but might have something to do with the robust power of this experimental design. Being a simple block-design task, the contrast maps generated in SPM often produce significant effect sizes and this increased power might help better discriminate between schizophrenia patients and controls. Also, the predominance of ICA features in our results show the benefit of including ICA component maps in data-fusion studies. Though there is some bias in the proportion of SPM features versus ICA features, functional connectivity maps generated by ICA represent an intrinsically different type of a biological marker. More specifically, the mathematical constraints of the GLM model prevent its feature maps to make any inferences regarding functional connectivity. Furthermore, a number of fMRI studies seem to suggest that schizophrenia might be better characterized by the aberrant connectivity of its brain regions rather than any localized deficit in one area of the brain (Friston 1999). This is not to say that the GLM is ineffective in elucidating the pathophysiology of schizophrenia, but that a complimentary approach using ICA might aid in the search for a meaningful biological marker. There are some limitations to our study that we would like to address. Our first limitation concerns task performance differences, especially in the SIRP task where patients statistically performed worse than controls. Even though this task was relatively simple in comparison to other N-back WM tasks, the well known difficulty in finding schizophrenia patients to perform this task at the same level as controls required us to make some sacrifices in order to increase our sample size. However, it is important to note that the mean average accuracy for both groups was greater than 95% and though there were statistical differences, both groups performed the task, on average, successfully. IQ was also not matched between groups, though patients with schizophrenia show significant differences in IQ versus matched controls. Some studies have attempted to account for this difference in IQ by using it as a covariate in their analyses, but reduced IQ has been known to represent an early manifestation of schizophrenia (Groom et al. 2008) and including this as a covariate might remove some of the interesting variability associated with the disease (Schwarz 1971). Furthermore, site differences were not taken into account when applying our particular analyses and scanner variability has been an issue concerning multi-site studies (Friedman and Glover 2006; Friedman et al. 2007), though these studies were performed with often small sample sizes ($N=5$). We hoped that the inclusion of multiple runs per experimental paradigm and our large sample size would mediate some of the variability issues seen in those previous multi-site studies. Finally, the medication history of patients with schizophrenia was not fully accounted for during this study. Patients were evaluated with schizophrenia and stabilized with medication by a licensed physician, but a full detailed history would allow us to account for some possible confounds associated with these medications.

Conclusion

Using a recently developed novel algorithm for data fusion, we were able to conglomerate a large number of fMRI features to determine potential biological markers in schizophrenia. However, one of the benefits of CCICA is its ability to use other types of features (such as fractional anisotropy maps or grey or white matter maps) which would allow for multimodal studies of schizophrenia among other disorders. Furthermore, CCICA was able to take advantage of the clinical diagnosis of each participant and use that to guide the extraction of

independent components to maximize between-group differences in its resulting components. The p-value metric we used allowed us to assess the degree to which the feature amplitude signals differed between patients and controls while the J-divergence metric allowed us to determine differences in the spatial distribution of that same signal. We found a striking consistency in our top p-value components that stemmed from the ICA SM frontal pole feature set. These components implicated the same bilateral frontal pole regions found from the original feature map and points to these regions as significant markers for pathology. The J-divergence results were more heterogeneous, but marked a set of regions that have been well implicated in previous fMRI studies of schizophrenia. Finally, the results are also consistent with a large number of structural MRI studies that show grey matter volume differences in these regions for schizophrenia patients. The analysis suggests that a significant biological marker for schizophrenia might be related to the functional modulation of a bilateral frontal pole network along with regions in the bilateral temporal lobes and parietal lobules.

Acknowledgments

This work was supported by the National Institutes of Health; Contract grant number: 1 RO1 EB 006841. We would like to personally thank Christopher Abbott for his insightful comments on this manuscript.

References

- Andreasen, NC., editor. Scale for the Assessment of Negative Symptoms (SANS). Iowa City: University of Iowa; 1983.
- Andreasen, NC., editor. Scale for the Assessment of Positive Symptoms (SAPS). Iowa City: University of Iowa; 1984.
- Antonova E, Kumari V, Morris R, Halari R, Anilkumar A, Mehrotra R, et al. The relationship of structural alterations to cognitive deficits in schizophrenia: a voxel-based morphometry study. *Biological Psychiatry*. 2005; 58(6):457–467. [PubMed: 16039619]
- Barta PE, Pearlson GD, Powers RE, Richards SS, Tune LE. Auditory hallucinations and smaller superior temporal gyral volume in schizophrenia. *The American Journal of Psychiatry*. 1990; 147(11):1457–1462. [PubMed: 2221156]
- Beckmann CF, DeLuca M, Devlin JT, Smith SM. Investigations into resting-state connectivity using independent component analysis. *Philosophical Transactions of the Royal Society of London. Series B: Biological Sciences*. 2005; 360(1457):1001–1013.
- Bell AJ, Sejnowski TJ. An information-maximization approach to blind separation and blind deconvolution. *Neural Computation*. 1995; 7(6):1129–1159. [PubMed: 7584893]
- Broyd SJ, Demanuele C, Debener S, Helps SK, James CJ, Sonuga-Barke EJ. Default-mode brain dysfunction in mental disorders: A systematic review. *Neuroscience and Biobehavioral Reviews*. 2008
- Calhoun VD, Adali T, Pearlson GD, Pekar JJ. A Method for Making Group Inferences from Functional MRI Data Using Independent Component Analysis. *Human Brain Mapping*. 2001; 14(3):140–151. [PubMed: 11559959]
- Calhoun VD, Adali T, Giuliani NR, Pekar JJ, Kiehl KA, Pearlson GD. Method for multimodal analysis of independent source differences in schizophrenia: combining gray matter structural and auditory oddball functional data. *Human Brain Mapping*. 2006; 27(1):47–62. [PubMed: 16108017]
- Calhoun VD, Kiehl KA, Pearlson GD. Modulation of temporally coherent brain networks estimated using ICA at rest and during cognitive tasks. *Hum Brain Mapp*. 2007a In Press.
- Calhoun VD, Maciejewski PK, Pearlson GD, Kiehl KA. Temporal lobe and “default” hemodynamic brain modes discriminate between schizophrenia and bipolar disorder. *Human Brain Mapping*. 2007b
- Calhoun VD, Kiehl KA, Pearlson GD. Modulation of temporally coherent brain networks estimated using ICA at rest and during cognitive tasks. *Human Brain Mapping*. 2008

- Caprihan A, Pearlson GD, Calhoun VD. Application of principal component analysis to distinguish patients with schizophrenia from healthy controls based on fractional anisotropy measurements. *Neuroimage*. 2008; 42(2):675–682. [PubMed: 18571937]
- Davidson LL, Heinrichs RW. Quantification of frontal and temporal lobe brain-imaging findings in schizophrenia: a meta-analysis. *Psychiatry Research*. 2003; 122(2):69–87. [PubMed: 12714172]
- Ford JM. Schizophrenia: the broken P300 and beyond. *Psychophysiology*. 1999; 36(6):667–682. [PubMed: 10554581]
- Freire L, Roche A, Mangin JF. What is the best similarity measure for motion correction in fMRI time series? *IEEE Transactions on Medical Imaging*. 2002; 21(5):470–484. [PubMed: 12071618]
- Friedman L, Glover GH. Reducing interscanner variability of activation in a multicenter fMRI study: controlling for signal-to-fluctuation-noise-ratio (SFNR) differences. *Neuroimage*. 2006; 33(2):471–481. [PubMed: 16952468]
- Friedman L, Stern H, Brown GG, Mathalon DH, Turner J, Glover GH, et al. Test-retest and between-site reliability in a multicenter fMRI study. *Human Brain Mapping*. 2007
- Friston, K. Statistical parametric mapping. 1994.
- Friston KJ. Schizophrenia and the disconnection hypothesis. *Acta Psychiatrica Scandinavica Supplementum*. 1999; 395:68–79. [PubMed: 10225335]
- Garrity AG, Pearlson GD, McKiernan K, Lloyd D, Kiehl KA, Calhoun VD. Aberrant “default mode” functional connectivity in schizophrenia. *The American Journal of Psychiatry*. 2007; 164(3):450–457. [PubMed: 17329470]
- Glahn DC, Ragland JD, Abramoff A, Barrett J, Laird AR, Bearden CE, et al. Beyond hypofrontality: a quantitative meta-analysis of functional neuroimaging studies of working memory in schizophrenia. *Human Brain Mapping*. 2005; 25(1):60–69. [PubMed: 15846819]
- Goldman-Rakic PS. Working memory dysfunction in schizophrenia. *The Journal of Neuropsychiatry and Clinical Neurosciences*. 1994; 6(4):348–357. [PubMed: 7841806]
- Goldman-Rakic PS, Selemon LD. Functional and anatomical aspects of prefrontal pathology in schizophrenia. *Schizophrenia Bulletin*. 1997; 23(3):437–458. [PubMed: 9327508]
- Groom MJ, Jackson GM, Calton TG, Andrews HK, Bates AT, Liddle PF, et al. Cognitive deficits in early-onset schizophrenia spectrum patients and their non-psychotic siblings: a comparison with ADHD. *Schizophrenia Research*. 2008; 99(1–3):85–95. [PubMed: 18083349]
- Hill K, Mann L, Laws KR, Stephenson CM, Nimmo-Smith I, McKenna PJ. Hypofrontality in schizophrenia: a meta-analysis of functional imaging studies. *Acta Psychiatrica Scandinavica*. 2004; 110(4):243–256. [PubMed: 15352925]
- Himberg J, Hyvarinen A, Esposito F. Validating the independent components of neuroimaging time series via clustering and visualization. *Neuroimage*. 2004; 22(3):1214–1222. [PubMed: 15219593]
- Kiehl KA, Stevens M, Laurens KR, Pearlson GD, Calhoun VD, Liddle PF. An adaptive reflexive processing model of neurocognitive function: Supporting evidence from a large scale ($n=100$) fMRI study of an auditory oddball task. *Neuroimage*. 2005a; 25:899–915. [PubMed: 15808990]
- Kiehl KA, Stevens MC, Celone K, Kurtz M, Krystal JH. Abnormal hemodynamics in schizophrenia during an auditory oddball task. *Biological Psychiatry*. 2005b; 57(9):1029–1040. [PubMed: 15860344]
- Kim DI, Manoach DS, Mathalon DH, Turner JA, Mannell M, Brown GG, et al. Dysregulation of working memory and default-mode networks in schizophrenia using independent component analysis, an fBIRN and MCIC study. *Human Brain Mapping*. 2009a
- Kim DI, Mathalon DH, Ford JM, Mannell M, Turner JA, Brown GG, et al. Auditory Oddball Deficits in Schizophrenia: An Independent Component Analysis of the fMRI Multisite Function BIRN Study. *Schizophrenia Bulletin*. 2009b; 35(1):67–81. [PubMed: 19074498]
- Kindermann SS, Karimi A, Symonds L, Brown GG, Jeste DV. Review of functional magnetic resonance imaging in schizophrenia. *Schizophrenia Research*. 1997; 27(2–3):143–156. [PubMed: 9416644]
- Laurens KR, Kiehl KA, Ngan ET, Liddle PF. Attention orienting dysfunction during salient novel stimulus processing in schizophrenia. *Schizophrenia Research*. 2005; 75(2–3):159–171. [PubMed: 15885507]

- Lee J, Park S. Working memory impairments in schizophrenia: a meta-analysis. *Journal of Abnormal Psychology*. 2005; 114(4):599–611. [PubMed: 16351383]
- Li YO, Adali T, Calhoun VD. Estimating the number of independent components for functional magnetic resonance imaging data. *Human Brain Mapping*. 2007; 28(11):1251–1266. [PubMed: 17274023]
- Machado G, Juarez M, Clark VP, Gollub RL, Magnotta V, White T, et al. Probing schizophrenia with a sensorimotor task: Large-scale ($n=273$) independent component analysis of first episode and chronic schizophrenia patients. 2007
- Manoach DS. Prefrontal cortex dysfunction during working memory performance in schizophrenia: reconciling discrepant findings. *Schizophrenia Research*. 2003; 60(2–3):285–298. [PubMed: 12591590]
- Manoach DS, Gollub RL, Benson ES, Searl MM, Goff DC, Halpern E, et al. Schizophrenic subjects show aberrant fMRI activation of dorsolateral prefrontal cortex and basal ganglia during working memory performance. *Biological Psychiatry*. 2000; 48(2):99–109. [PubMed: 10903406]
- Meda SA, Bhattarai M, Morris NA, Astur RS, Calhoun VD, Mathalon DH, et al. An fMRI study of working memory in first-degree unaffected relatives of schizophrenia patients. *Schizophrenia Research*. 2008; 104(1–3):85–95. [PubMed: 18678469]
- Meisenzahl EM, Koutsouleris N, Bottlender R, Scheuerecker J, Jager M, Teipel SJ, et al. Structural brain alterations at different stages of schizophrenia: a voxel-based morphometric study. *Schizophrenia Research*. 2008; 104(1–3):44–60. [PubMed: 18703313]
- Meyer-Lindenberg A, Poline JB, Kohn PD, Holt JL, Egan MF, Weinberger DR, et al. Evidence for abnormal cortical functional connectivity during working memory in schizophrenia. *The American Journal of Psychiatry*. 2001; 158(11):1809–1817. [PubMed: 11691686]
- Minzenberg MJ, Laird AR, Thelen S, Carter CS, Glahn DC. Meta-analysis of 41 functional neuroimaging studies of executive function in schizophrenia. *Archives of General Psychiatry*. 2009; 66(8):811–822. [PubMed: 19652121]
- Park HJ, Levitt J, Shenton ME, Salisbury DF, Kubicki M, Kikinis R, et al. An MRI study of spatial probability brain map differences between first-episode schizophrenia and normal controls. *Neuroimage*. 2004; 22(3):1231–1246. [PubMed: 15219595]
- Pearlson GD. Superior temporal gyrus and planum temporale in schizophrenia: a selective review. *Progress in Neuropsychopharmacology & Biological Psychiatry*. 1997; 21(8):1203–1229.
- Quintana J, Wong T, Ortiz-Portillo E, Kovalik E, Davidson T, Marder SR, et al. Prefrontal-posterior parietal networks in schizophrenia: primary dysfunctions and secondary compensations. *Biological Psychiatry*. 2003; 53(1):12–24. [PubMed: 12513941]
- Schneider F, Habel U, Reske M, Kellermann T, Stocker T, Shah NJ, et al. Neural correlates of working memory dysfunction in first-episode schizophrenia patients: an fMRI multi-center study. *Schizophrenia Research*. 2007; 89(1–3):198–210. [PubMed: 17010573]
- Schroder J, Essig M, Baudendistel K, Jahn T, Gerdson I, Stockert A, et al. Motor dysfunction and sensorimotor cortex activation changes in schizophrenia: A study with functional magnetic resonance imaging. *Neuroimage*. 1999; 9(1):81–87. [PubMed: 9918729]
- Schwarz JC. High School Yearbooks: Further explication and reply to Meehl. *Journal of Abnormal Psychology*. 1971; 78(2):145–147. [PubMed: 5156439]
- Sternberg S. High-speed scanning in human memory. *Science*. 1966; 153(736):652–654. [PubMed: 5939936]
- Sui J, Adali T, Pearlson GD, Calhoun VD. An ICA-based method for the identification of optimal FMRI features and components using combined group-discriminative techniques. *Neuroimage*. 2009a; 46(1):73–86. [PubMed: 19457398]
- Sui J, Adali T, Pearlson GD, Clark VP, Calhoun VD. A method for accurate group difference detection by constraining the mixing coefficients in an ICA framework. *Human Brain Mapping*. 2009b
- Xu L, Groth KM, Pearlson G, Schretlen DJ, Calhoun VD. Source-based morphometry: the use of independent component analysis to identify gray matter differences with application to schizophrenia. *Human Brain Mapping*. 2009; 30(3):711–724. [PubMed: 18266214]

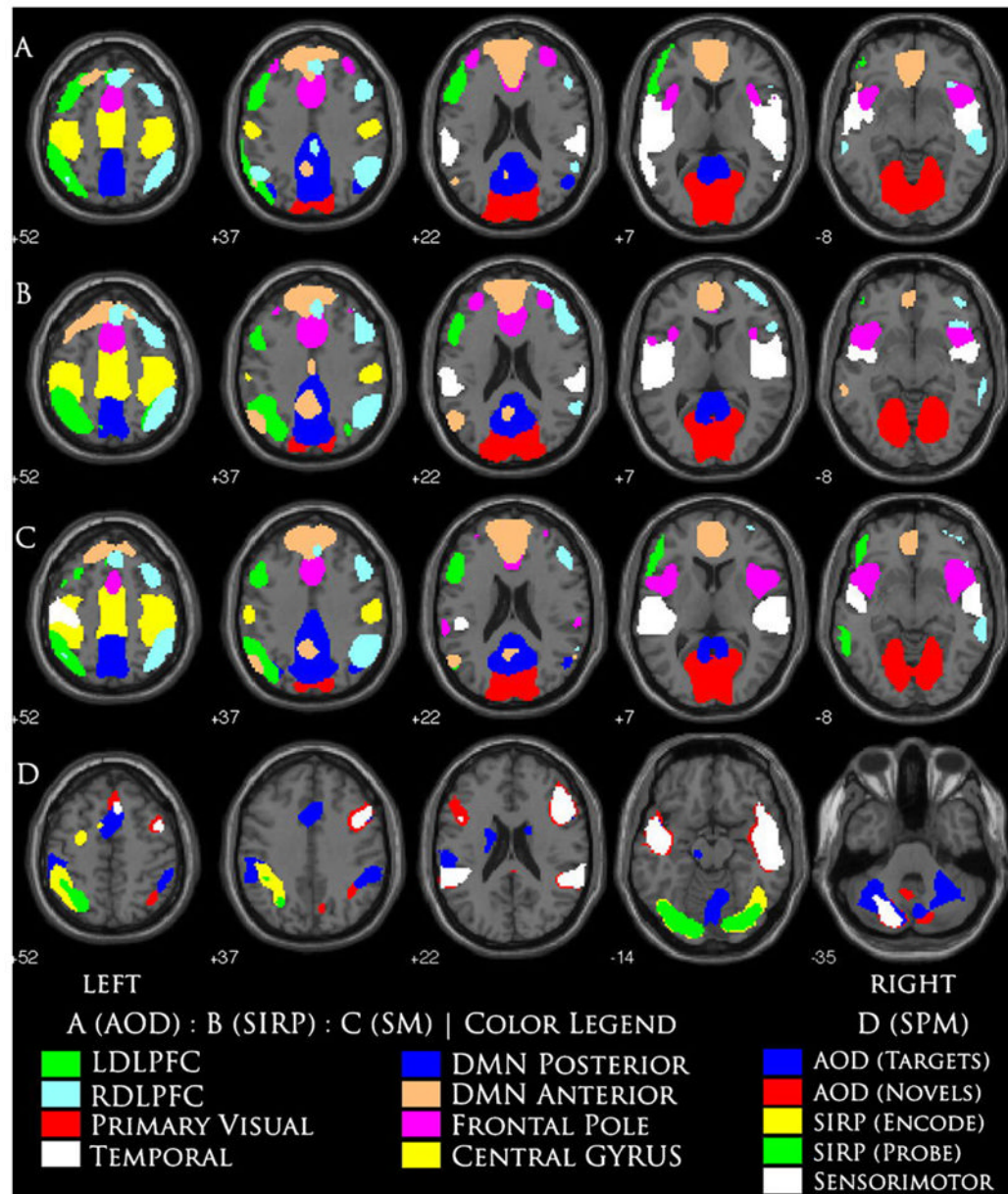
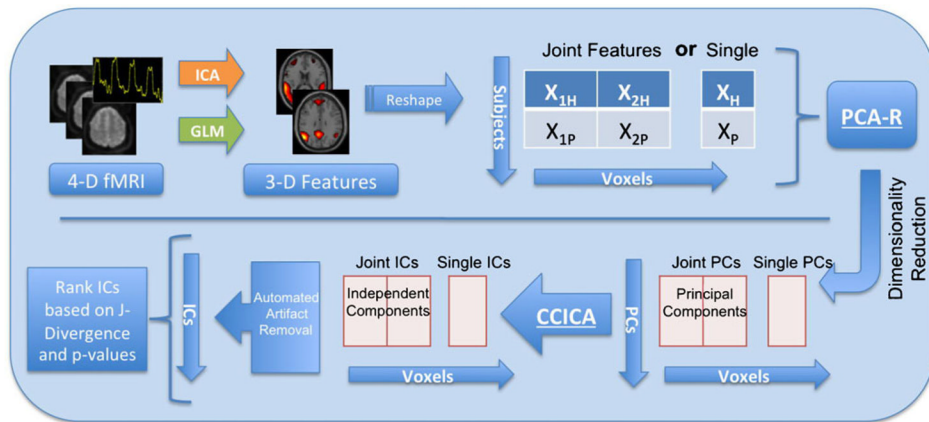


Fig. 1. Overlay of 29 features from ICA and GLM approaches. The first three rows represent ICA features from different tasks where the rows from top to bottom are AOD, SIRP, and SM task respectively. The ICA features have all been thresholded at the same t-threshold (FDR, $p < 1 \times 10^{-12}$), while the SPM overlays (fourth row) have been thresholded at various p-values beyond FDR, $p < 1 \times 10^{-4}$ for display purposes

**Fig. 2.**

An overview of the CCICA analysis starting from the preprocessed fMRI data and ending with the ranked CCICA components by J-divergence and p-values. fMRI data is first preprocessed to undergo analysis via ICA and GLM. This results in a set of features that are no longer time-dependent and reshaped into a matrix of subjects by voxels. A further data reduction step takes place via PCA-R which allows us to prepare our data for CCICA. The CCICA then extracts its own set of independent components that might contain single or joint feature components based off of the individual features themselves and all possible pairwise comparisons of these features. Finally an automated artifact removal tool allows us to find components related to areas of the brain only and we rank these components based off of their j-divergence and p-value results

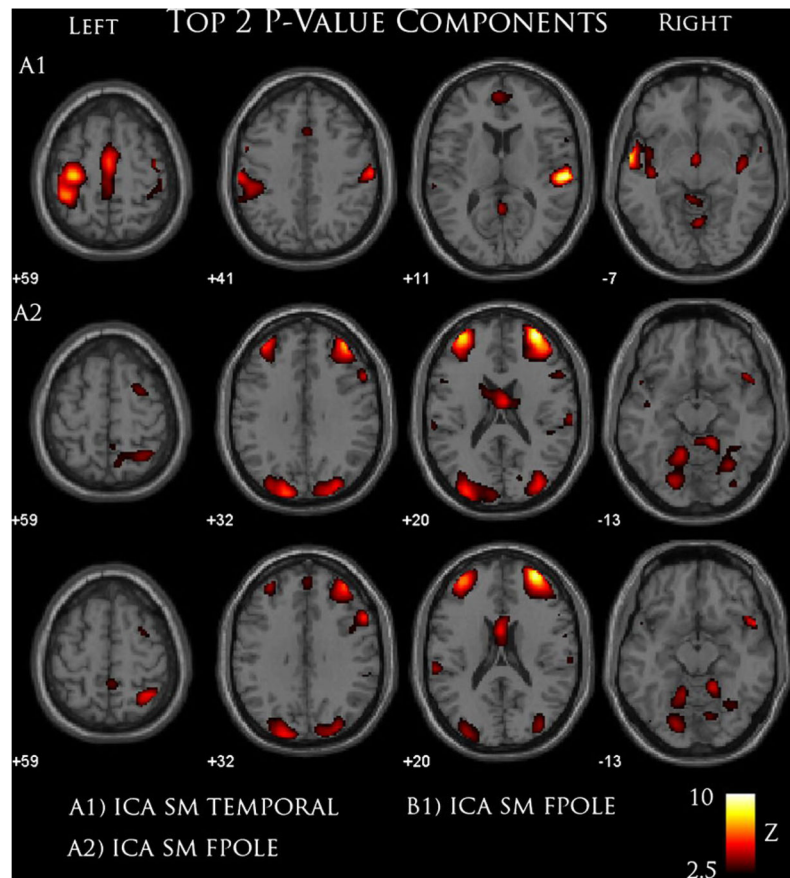


Fig. 3. Results from the top 2 components ranked by their p-value metrics. All maps have been thresholded at $z\text{-score} > 2.5$ and the highest ranked components are shown from top to bottom. A high p-value ranking reflects a significant difference in the amplitude or modulation of their fMRI signal within the context of their associated feature component

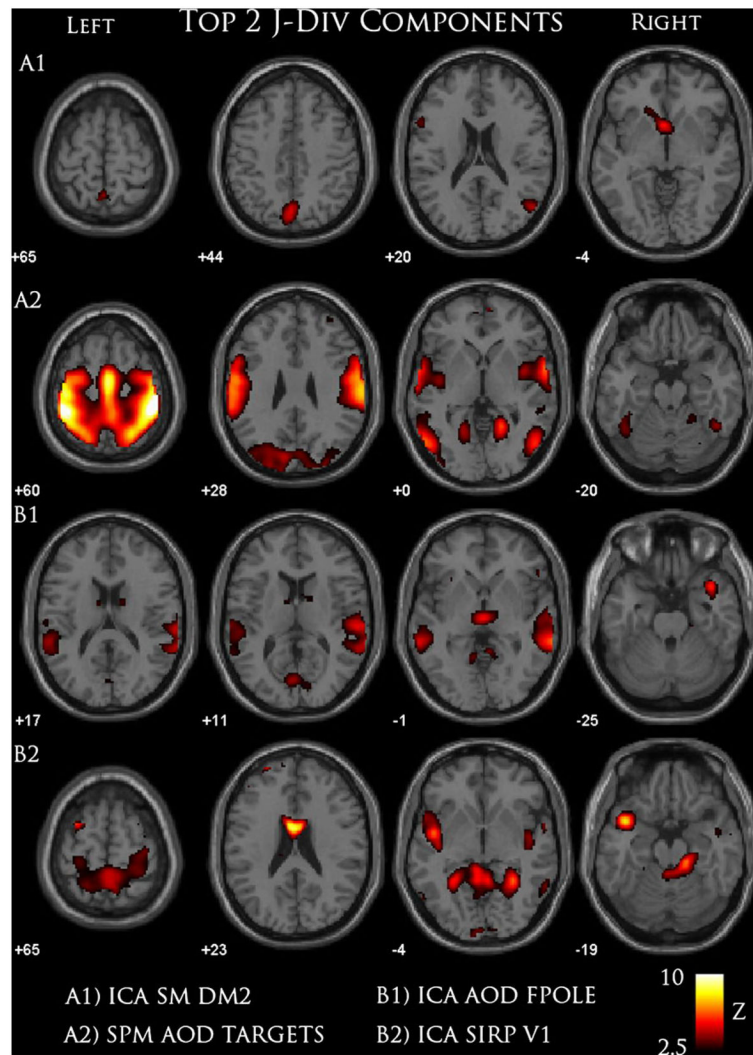


Fig. 4. Results from the top 2 components ranked by their J-divergence metrics. All maps have been thresholded at $z\text{-score} > 2.5$ and the highest ranked components are shown from top to bottom. The J-divergence metric determines the degree of spatial heterogeneity between patients and controls, where a high J-divergence score reflects significant differences in the distribution of their feature component signals

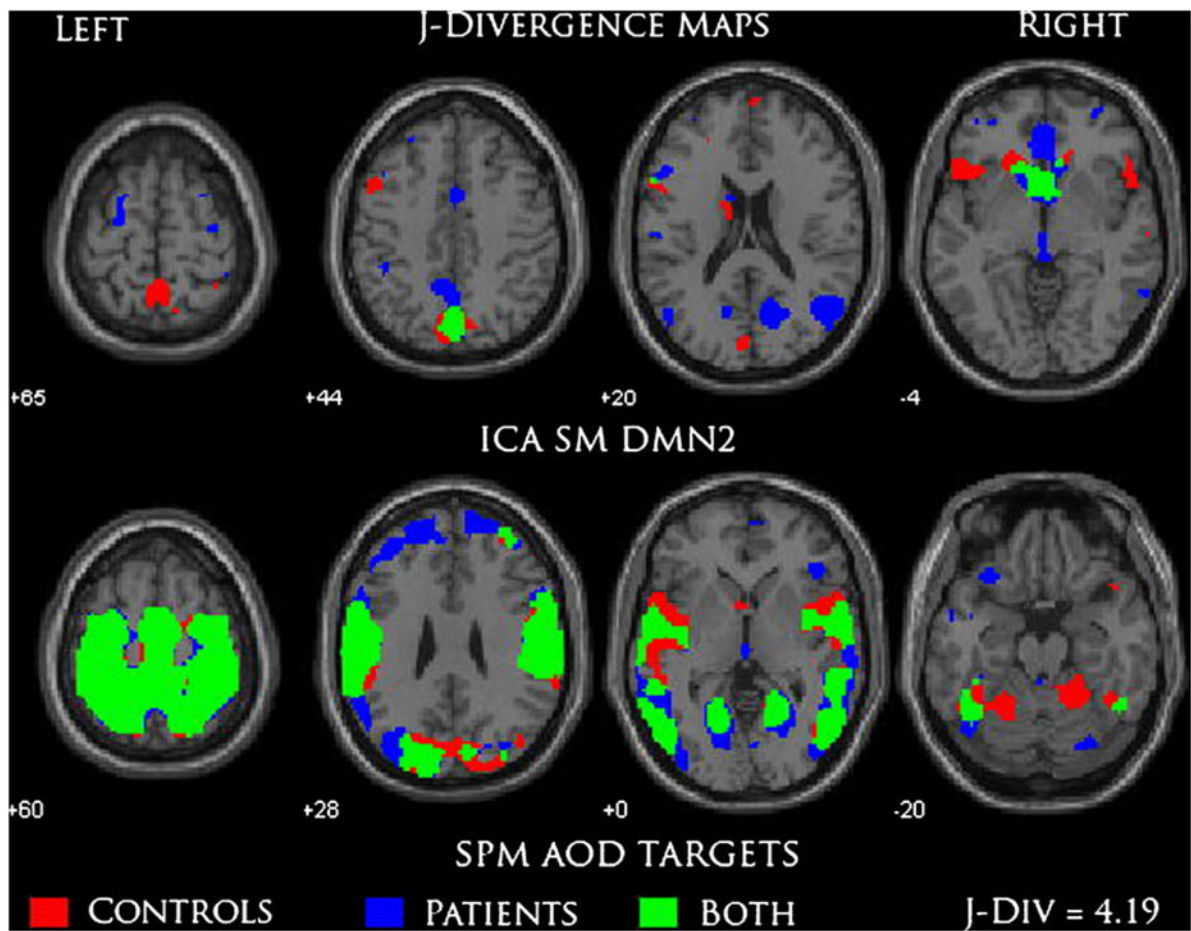


Fig. 5.

A closer look at the J-divergence metric for the highest scoring CCICA component. The regions reflect z-scores greater than 2.5 for patients, controls, and both. The region in green shows where both participant groups had z-scores greater than 2.5 and the degree of spatial variability can be seen in the number of regions that are not shared between both groups

Table 1

Demographics and patient SANS-SAPS including age, gender, handedness, education, paternal education, maternal education, and WRAT intelligence measures. SANS and SAPS scores for patients with schizophrenia are also included in this table

Feature Description	Labels	Feature Type	Tasks
Left dorsal lateral prefrontal cortex	LDLPFC	ICA Component Map	AOD,SIRP,SM
Right dorsal lateral prefrontal cortex	RDLPFC	ICA Component Map	AOD,SIRP,SM
Primary Visual	V1	ICA Component Map	AOD,SIRP,SM
Bilateral Temporal	Temporal	ICA Component Map	AOD,SIRP,SM
Default Mode Network Posterior	DMN1	ICA Component Map	AOD,SIRP,SM
Default Mode Network Anterior	DMN2	ICA Component Map	AOD,SIRP,SM
Bilateral Frontal Pole	FPOLE	ICA Component Map	AOD,SIRP,SM
Pre/Post Central Gyrus	Central	ICA Component Map	AOD,SIRP,SM
Targets vs. Standards	Targets	SPM Contrast Map	AOD
Novels vs. Standards	Novels	SPM Contrast Map	AOD
Encode Block Average	Encode	SPM Contrast Map	SIRP
Probe Block Average	Probe	SPM Contrast Map	SIRP
Motor Tapping Block Average	Motor	SPM Contrast Map	SM

Table 2

Feature labels and their associated descriptions while multiple paradigms under the tasks column imply the particular feature existed for those tasks. Labels refer to the abbreviation for each feature used during the results and discussion section. Feature type defines whether it originated from an ICA or GLM analysis. Note, not all regions that are activated are defined in the feature description

Demographics				
	<i>Age in Years (n=154)</i>	<i>Gender (n=154)</i>	<i>Handedness (n=152)</i>	
Controls	30.70/11.30 (<i>M/SD</i>)	M=54/F=32	Right=78/L=3/B=4	
Patients	31.85/11.35	M=55/F=13	Right=60/L=4/B=2	
2-Sample t-test	$t=-.6289/p=.5304$	Male/Female	Right/Left/Both	
Education & Intelligence				
	<i>Education (n=152)</i>	<i>Paternal Edu (n=142)</i>	<i>Maternal Edu (n=147)</i>	<i>WRAT (n=149)</i>
Controls	15.24/2.06 (<i>M/SD</i>)	14.87/3.36	13.98/2.60	51.19/3.73
Patients	13.72/2.44	14.46/3.86	13.83/3.73	48.13/5.51
2-Sample t-test	$t=4.1521/p<.0001$	$t=.6738/p=.5015$	$t=.2886/p=.7733$	$t=4.0397/p<.0001$
Positive & Negative Syndrom Scales				
	<i>SANS (n=67)</i>		<i>SAPS (n=67)</i>	
Affect	1.43/1.16 (<i>M/SD</i>)	Hallucinations	2.31/1.66	
Alogia	.82/1.08	Delusions	2.46/1.39	
Avolition	2.60/1.39	Bizarre Behavior	.90/1.10	
Anhedonia	2.54/1.25	Thought Disorder	.97/1.23	
Attention	1.63/1.30			

Behavioral results from the AOD and SIRP task. Between patients and controls, no significant differences were seen in the percent accuracy for correct responses, reaction time, number of misses for the AOD task. Significant differences were seen in this task for the number of incorrect responses. For the SIRP task, significant differences were seen in the overall load accuracy, low load, medium load, and high load. No significant differences were seen in the reaction time for this task

Table 3

Auditory Oddball Performance Statistics			
	Overall Accuracy(%)	AOD Reaction(ms)	AOD #Misses
Controls ($n=86$)	93.770/7.201 (M/SD)	529.831/133.275	.66/1.28
Patients ($n=68$)	94.818/6.184	525.908/105.678	.75/1.36
2-Sample t-test	$t=-.9357/p=.3417$	$t=-.1984/p=.843$	$t=-.4078/p=.684$
Sternberg Item Recognition Paradigm Performance Statistics			
	Overall Accuracy(%)	SIRP Reaction(ms)	AOD #Incorrects
Controls ($n=86$)	98.606/.999 (M/SD)	690.629/129.755	1.71/2.21
Patients ($n=68$)	96.567/3.133	720.296/119.750	2.82/3.47
2-Sample t-test	$t=5.6855/p<.0001$	$t=1.4573, p=.1471$	$t=-2.422/p=.0166$
	Load 1 Accuracy	Load 2 Accuracy	Load 3 Accuracy
Controls ($n=86$)	99.152/1.083	98.625/1.514	98.041/1.837
Patients ($n=68$)	98.484/2.072	95.821/4.643	95.379/4.669
2-Sample t-test	$t=2.5777/p=.0109$	$t=5.2617/p<.0001$	$t=4.8397/p<.0001$

Table 4

Top 10 components by p-value (top) and J-divergence (bottom)

	J-Divergence	Component	P-Value	T-values
Top P-value Components				
ICA sm TEMPORAL & ICA sm FPOLE	0.772	1	1.03E-15	-8.970
ICA sm FPOLE	0.508	1	2.77E-14	-8.410
ICA sirp FPOLE & ICA sm FPOLE	0.505	1	1.17E-12	-7.758
ICA aod V1 & ICA sm FPOLE	1.990	1	1.60E-12	-7.702
ICA sirp V1 & ICA sm FPOLE	0.052	1	1.99E-12	-7.663
ICA aod V1 & ICA sm FPOLE	0.580	2	1.60E-09	6.425
ICA sirp V1 & ICA sm FPOLE	0.045	2	1.28E-07	5.543
ICA aod TEMPORAL & ICA sm FPOLE	0.087	2	6.32E-06	4.679
ICA sm FPOLE & SPM aod nov std	0.669	2	5.00E-05	-4.175
ICA sirp TEMPORAL & ICA sm FPOLE	0.258	2	2.27E-04	3.777
Top J-divergence Components				
ICA sm DMN2 & SPM aod targ std	4.188	2	8.79E-04	-3.394
ICA aod FPOLE & ICA sirp V1	3.988	12	9.00E-01	-0.126
ICA sm V1	3.693	9	2.54E-01	-1.145
ICA sirp DMN1	3.529	9	2.95E-01	-1.051
ICA aod TEMPORAL & ICA aod DMN2	3.273	11	6.60E-01	-0.441
ICA aod FPOLE & ICA aod DMN2	2.750	4	8.69E-03	-2.658
ICA sm TEMPORAL	2.732	1	6.11E-06	-4.687
ICA aod TEMPORAL & ICA sirp V1	2.720	1	2.15E-06	4.927
ICA sm V1	2.646	1	1.12E-05	4.543
ICA aod DMN2 & ICA sm LDLPFC	2.624	1	1.79E-04	-3.842

Table 5

Talairach and Brodmann labels for the top p-value CCICA components. The top 5 regions are shown for each component, ordered by their area of activation

Talairach Labels	Brodmann Areas	R/L (mm ³)	(R/L) Max Z-Scores (MNI Coord.)
ICA SM Temporal & ICA SM Frontal Pole (SM Temporal)			
Precentral Gyrus	6, 4, 44, 3, 43	2.5/7.5	6.4(-59,-15,42)/10.9(33,-17,62)
Transverse Temporal Gyrus	41, 42	0.6/0.0	10.1(-56,-20,12)/2.8(62,-14,12)
Superior Temporal Gyrus	42, 41, 22, 21, 38, 13	3.0/6.2	10.0(-59,-20,12)/9.3(59,0,-3)
Middle Temporal Gyrus	21	0.1/1.2	3.3(-59,3,-8)/8.9(59,-3,-5)
Superior Frontal Gyrus	6, 11	0.5/0.9	4.3(-3,6,52)/8.3(27,-8,64)
ICA SM Temporal & ICA SM Frontal Pole (SM Frontal Pole)			
Caudate		3.1/2.8	17.3(-6,3,8)/16.1(6,3,8)
Anterior Cingulate	25	0.4/0.3	11.1(-3,6,-3)/10.9(3,6,-3)
Culmen		2.5/3.2	10.2(-3,-45,-20)/10.7(0,-39,-21)
Superior Frontal Gyrus	10, 9, 6	5.0/3.2	10.0(-33,56,14)/8.6(33,53,17)
Middle Frontal Gyrus	10, 46, 9, 6, 11, 8	14.5/6.2	9.3(-36,51,20)/8.7(33,51,20)
ICA SM Frontal Pole			
Caudate		2.8/2.4	15.1(-6,6,8)/15.0(6,3,8)
Anterior Cingulate	25, 24	0.6/0.3	10.8(-3,6,-3)/10.0(3,6,-3)
Superior Frontal Gyrus	10, 9	5.8/2.7	9.5(-33,56,17)/7.1(33,50,17)
Middle Frontal Gyrus	10, 46, 9, 6, 8	14.5/4.8	8.4(-33,53,19)/6.6(33,51,20)
Culmen		2.5/3.2	5.7(-15,-47,-5)/7.5(12,-53,-2)

Table 6

Talairach and Brodmann labels for the top J-Divergence CCICA components. The top 5 regions are shown for each component, ordered by their area of activation

Talairach Labels	Brodmann Areas	R/L (mm ³)	(R/L) Max Z-Scores (MNI Coord.)
ICA SM DMN2 & SPM AOD TARGETS (SM DMN2)			
Precuneus	7	2.6/2.3	11.1(-3,-65,42)/11.3(3,-68,42)
Middle Temporal Gyrus	39, 19	2.1/0.0	10.6(-50,-63,22)/-999.0(0,0,0)
Superior Temporal Gyrus	39, 22, 38	0.7/0.1	9.8(-56,-63,22)/8.8(36,13,-23)
Inferior Frontal Gyrus	44, 45, 47	0.2/1.3	8.7(-39,17,-16)/9.5(56,15,19)
Medial Frontal Gyrus	11, 10	0.3/0.2	8.8(-3,40,-17)/9.3(3,43,-15)
ICA SM DMN2 & SPM AOD TARGETS (AOD Targets)			
Postcentral Gyrus	2, 1, 3, 40, 5, 7, 43	21.7/18.8	12.1(-42,-35,60)/11.3(39,-35,60)
Inferior Parietal Lobule	40, 2	10.0/12.1	11.4(-45,-32,57)/10.8(48,-32,54)
Precentral Gyrus	4, 6, 43, 3, 44, 13, 9	25.6/22.2	11.2(-39,-23,62)/9.5(36,-20,62)
Superior Parietal Lobule	7, 5	4.5/4.5	9.6(-33,-47,60)/8.8(33,-47,60)
Medial Frontal Gyrus	6, 32, 10, 11	8.3/6.5	9.0(-3,-6,53)/8.0(3,-9,50)
ICA AOD Frontal Pole & ICA SIRP V1 (AOD Frontal Pole)			
Middle Temporal Gyrus	21, 22	6.1/4.6	10.7(-65,-38,2)/7.0(62,-38,2)
Superior Temporal Gyrus	41, 42, 22, 38, 13, 21	13.7/6.0	9.3(-39,13,-23)/6.0(56,-40,21)
Thalamus		1.4/1.6	8.0(-3,-15,1)/7.0(3,-15,1)
Postcentral Gyrus	40, 2, 43, 1, 3	1.6/0.4	6.2(-65,-25,18)/4.2(59,-20,15)
Insula	13	0.1/0.7	3.8(-50,-20,15)/5.8(56,-37,18)
ICA AOD Frontal Pole & ICA SIRP V1 (SIRP V1)			
Superior Temporal Gyrus	38, 22, 13, 41, 21	3.0/9.1	8.6(-45,-1,-10)/11.3(42,8,-18)
Middle Frontal Gyrus	6, 8, 10, 46, 9	2.0/4.5	9.3(-30,23,54)/10.5(30,15,57)
Postcentral Gyrus	5, 7, 2, 3, 1, 40, 43	5.4/4.2	10.4(-3,-46,66)/8.7(6,-43,66)
Superior Frontal Gyrus	10, 8, 9, 6	1.3/3.4	8.9(-33,26,51)/10.4(33,59,14)
Culmen		6.0/2.6	10.4(-15,-33,-16)/10.1(3,-41,-6)